

Tumor-Specific Positron Emission Tomography Imaging in Patients: [¹⁸F] Fluorodeoxyglucose and Beyond

David A. Mankoff, Janet F. Eary, Jeanne M. Link, Mark Muzi, Joseph G. Rajendran, Alexander M. Spence, and Kenneth A. Krohn

Abstract Biochemical and molecular imaging of cancer using positron emission tomography (PET) plays an increasing role in the care of cancer patients. Most clinical work to date uses the glucose analogue [¹⁸F]fluorodeoxyglucose (FDG) to detect accelerated and aberrant glycolysis present in most tumors. Although clinical FDG PET has been used largely to detect and localize cancer, more detailed studies have yielded biological insights and showed the utility of FDG as a prognostic marker and as a tool for therapeutic response evaluation. As cancer therapy becomes more targeted and individualized, it is likely that PET radiopharmaceuticals other than FDG, aimed at more specific aspects of cancer biology, will also play a role in guiding cancer therapy. Clinical trials designed to test and validate new PET agents will need to incorporate rigorous quantitative image analysis and adapt to the evolving use of imaging as a biomarker and will need to incorporate cancer outcomes, such as survival into study design.

Imaging plays an increasing role in the care of cancer patients (1). Anatomic imaging, such as plain radiography, computed tomography (CT), and magnetic resonance, is most commonly used to detect and localize cancer, where tumors are recognized and followed based on their density, shape, size, and location. More recently, functional, biochemical, and molecular imaging methods have been developed [e.g., [¹⁸F]fluorodeoxyglucose positron emission tomography (FDG PET)], which are complementary to anatomic imaging and are proving effective in guiding the care of cancer patients (1–4). This review highlights the application of PET using FDG and other tracers to cancer patients, with an emphasis on the unique capabilities of PET and its application to individualized and targeted cancer therapy. The ability to generate a wide variety of radiopharmaceuticals is a major strength of the PET approach (4, 5). Some newer PET imaging agents that have been tested in patients will also be reviewed.

To understand where biological imaging may play a role in caring for cancer patients, it is important to identify unmet diagnostic needs (6). These include (a) more accurate cancer detection and staging, (b) earlier and more predictive assessment of therapeutic response, and (c) better characterization of tumor biology for directing the choice and aggressiveness of therapy for the individual patient. For identifying and local-

izing cancer sites, biochemical imaging by PET can identify tumors based on features that are aberrantly expressed in the tumor compared with normal tissue and complementary to information from anatomic imaging. For example, the identification of regional lymph node metastases based on increased glucose metabolism with FDG PET, combined with anatomic imaging by CT, improves the accuracy of cancer staging compared with CT alone (7, 8). The complementary nature of PET and CT data led to the development of combined PET/CT devices, which can provide coregistered functional and anatomic information (9).

Biochemical and molecular imaging offers significant advantages in evaluating response to cancer treatment. The standard approach to assessing tumor response is based on a change in tumor size (10, 11). However, a decline in apparent tumor size is a relatively late event in response to cytotoxic cancer treatment (Fig. 1). It is preceded by biochemical and cellular changes that include a decrease in cell proliferation, an increase in cell death, and a decline in the number of viable tumor cells. These events can be detected by PET much earlier than tumor size changes are apparent (12–17). Furthermore, tumor bulk is not necessarily a reliable indication of the risk of tumor progression after therapy (18). Quantifying the residual tumor after therapy based on *in vivo* tumor biology, characterized regionally using biochemical and functional imaging, provides a more clinically relevant measure of response. Several studies have shown that PET imaging measures of response are highly predictive of patient outcomes, such as time-to-progression, disease-free survival, and overall survival, often out-performing size-based estimates of response (12, 13, 19–24).

Finally, characterization of tumor biology *in vivo* by molecular imaging may help to determine how aggressive a cancer is likely to be and how best to treat the cancer (25).

Authors' Affiliation: University of Washington and Seattle Cancer Care Alliance, Seattle, Washington

Received 1/12/07; revised 4/11/07; accepted 4/12/07.

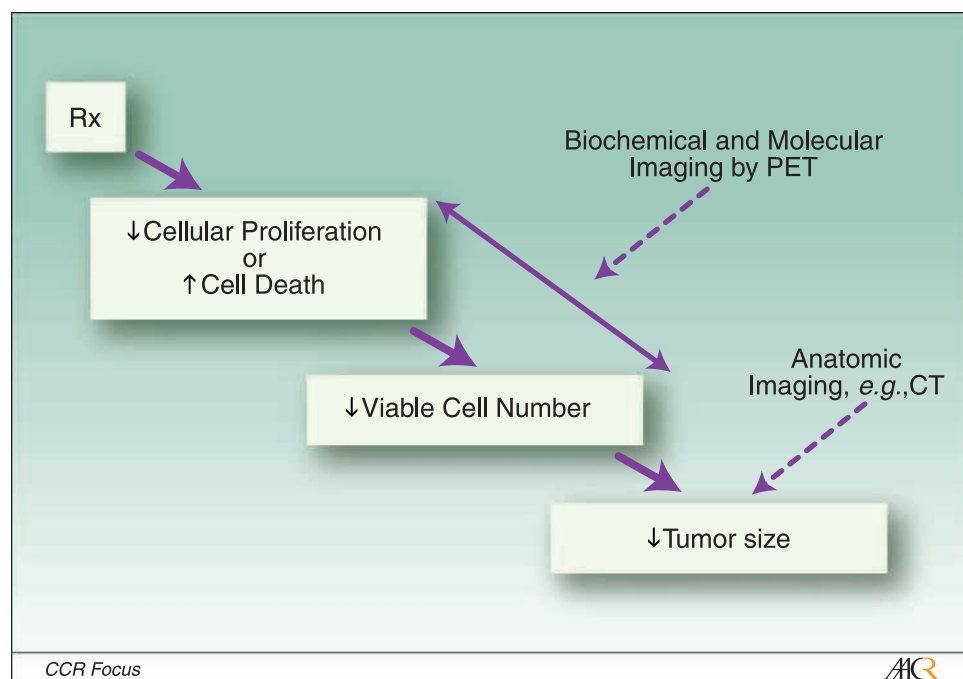
Grant support: NIH grants CA42045, CA72064, CA90771, and S10 RR17229.

Requests for reprints: David A. Mankoff, Box 356113, Room NN203, University of Washington Medical Center, 1959 NE Pacific Street, Seattle, WA 98195. Phone: 206-288-2173; E-mail: dam@u.washington.edu.

© 2007 American Association for Cancer Research.

doi:10.1158/1078-0432.CCR-07-0074

Fig. 1. Diagram of steps in cancer response. Dashed arrows, where PET and conventional can measure changes along the sequence of processes underlying tumor response.



Traditionally, prognostic assays have been done by *in vitro* assay of biopsy material. Molecular imaging data can be complementary to *in vitro* assays and provide information not possible by analysis of sampled material. Imaging is able to include all tumor sites in the imaging field of view and thus estimate tumor heterogeneity, which cannot be reliably measured in a limited biopsy. PET can image the effect of drugs on tumors *in vivo* because it can be done serially and noninvasively. As such, PET imaging can be used together with *in vitro* assays to guide the selection of cancer therapy (26). For example, recent studies have shown that FDG PET strongly predicts which iodine-refractory thyroid cancers are most likely to progress and lead to patient death and identifies which patients need aggressive treatment (27). This prediction is not possible by analysis of thyroid cancer histology. In addition, PET imaging may help identify appropriate targets for treatment. For example, PET imaging of estrogen receptors (ER) in breast cancer using [¹⁸F]fluoroestradiol (FES) PET can identify regional ER expression and predict response to endocrine therapy (28, 29). These are but a few illustrations of how imaging can complement assay of tissue samples in directing targeted cancer therapy.

FDG PET for Cancer Imaging

Underlying biology and approach. The development of FDG dates to the work of Sokoloff et al. (30), who developed a method to measure the regional cerebral glucose metabolic rate in animals using [¹⁴C]deoxyglucose autoradiography. Subsequently, [¹⁸F]FDG was developed to provide the same capability using PET imaging to quantify the regional concentration of the ¹⁸F label in humans (31, 32). FDG is transported into cells and phosphorylated to FDG-6P by hexokinase in

parallel to glucose; however, the presence of an F atom instead of a hydroxyl group at the C2-position prevents FDG-6P from being a substrate for enzymes further down the glycolytic pathway. In most tissues, FDG-6P is trapped in cells and provides an indication of metabolic rate. There is evidence that FDG-6P can be slowly dephosphorylated in some tissues and tumors, especially those that break down glycogen or synthesize glucose as part of their normal function, such as liver and brain, where dephosphorylation is required (31, 33).

The most detailed method for quantifying regional glucose metabolism uses dynamic PET imaging to capture the tissue uptake curve for 60 to 90 min after injection with blood sampling or imaging of a blood pool to measure the blood clearance curve (22, 34). A compartmental model (Fig. 2) applied to these data provides accurate estimates of physiologic rate constants. The metabolic rate of glucose measured by FDG PET, sometimes termed the metabolic rate of FDG, is calculated from the flux of FDG from the blood to the phosphorylated state, as shown in Fig. 2A (22, 34). Metabolic rate of FDG is then estimated by the following: metabolic rate of FDG = [Glucose] K_i , where [Glucose] is the plasma glucose concentration (mmoles/mL), K_i is the flux constant from compartmental analysis (mL/min/g), and metabolic rate of FDG is quantified as mmoles/min/g. This analysis does not assume a value for relative glycolytic flux of FDG and glucose, the so-called "lumped constant" used in the original Sokoloff formulation (30), but rather describes glucose metabolic rate as assessed using FDG (33).

In clinical practice, dynamic imaging is time consuming and difficult to do over extended imaging fields covering the body. Most centers capture a single image of FDG uptake 60 min after injection as an approximate indication of glucose metabolism (35). From this static uptake image, a simplified uptake measure, usually known as the standardized uptake

value (SUV) can be calculated as (34) $SUV = C_t / (i.d. / wt)$, where C_t is the tissue FDG uptake from the image (mCi/mL or mCi/g), i.d. is injected dose (mCi), and wt is the patient weight (kg). Depending on the units for uptake from the scanner, the SUV will be unitless or have density units (g/mL). A SUV = 1 indicates uniform distribution of tracer, whereas SUV > 1 indicates accumulation. Tumors have considerably variable uptake, but generally untreated tumors have maximum SUVs of 3 or higher (36).

The use of FDG as a tumor detection agent is based on the observation of Warburg (37) in the 1930s that cancer cells have aberrantly high rates of glycolysis. The regulation of this process is complex, and a large number of factors and possible metabolic fates of glucose all influence the flux through the glycolytic pathway measured by FDG (Fig. 2B). Some glucose is used for biosynthesis via the pentose shunt; however, this seems to account for a relatively small fraction of glucose use in tumors (38). Tumor hypoxia may lead to anaerobic glycolysis and an increased rate of FDG metabolism (39). However, much of the increase in glucose use in tumors seems to be related to accelerated flux through the glycolytic pathway, even under aerobic conditions (40). An increased understanding of the molecular pathways active in cancer cells suggests that key molecules involved in accelerated cellular proliferation (e.g., mitogen-activated protein kinase) and decreased apoptosis, such as AKT, may be responsible for an elevated glucose consumption that relies heavily on aerobic glycolysis compared with normal tissues (41–44). Some authors have suggested that aberrant glycolysis dampens the apoptotic response to the metabolic stresses of uncontrolled proliferation and is essential to the cancer phenotype (40, 44, 45).

In addition to elevated glycolysis, tumors have differing and often increased expression of glucose transporters and/or hexokinase compared with normal tissues (40). This effect contributes to variable selectivity of FDG versus glucose in tumors compared with normal tissue, making the lumped constant variable in tumors, but there is generally higher FDG uptake relative to glucose in tumor than in normal tissues (46). There is some debate as to the relative importance of glucose transporters versus hexokinase activity in determining the level of FDG uptake in tumors (47); however, data from both *in vitro* (40) and *in vivo* studies (48) suggest that phosphorylation, and not membrane transport, is rate controlling in most circumstances.

Several features have contributed to the widespread use of FDG in the clinic (3). FDG, unlike glucose, is filtered in the kidneys, leading to substantial clearance from the blood pool by 1 h after injection. The enzyme responsible for FDG retention, hexokinase, is plentiful and highly active, effectively trapping the label in a short period after transport from the blood or tissue. This combination of high target tissue uptake and rapid blood clearance results in high-contrast images using short-lived radiopharmaceuticals. Metabolism of FDG beyond FDG-6P is minimal; therefore, there are few labeled metabolites in the blood. There is just enough background uptake of FDG to provide an “anatomic backdrop” to reference tumor location without interfering with the ability to visualize tumors. Finally, the nearly 2-h half-life of ^{18}F permits regional supply of FDG from a central facility. All these factors contribute to the

desirability of FDG as a clinical cancer imaging agent and to its increasing use in cancer imaging.

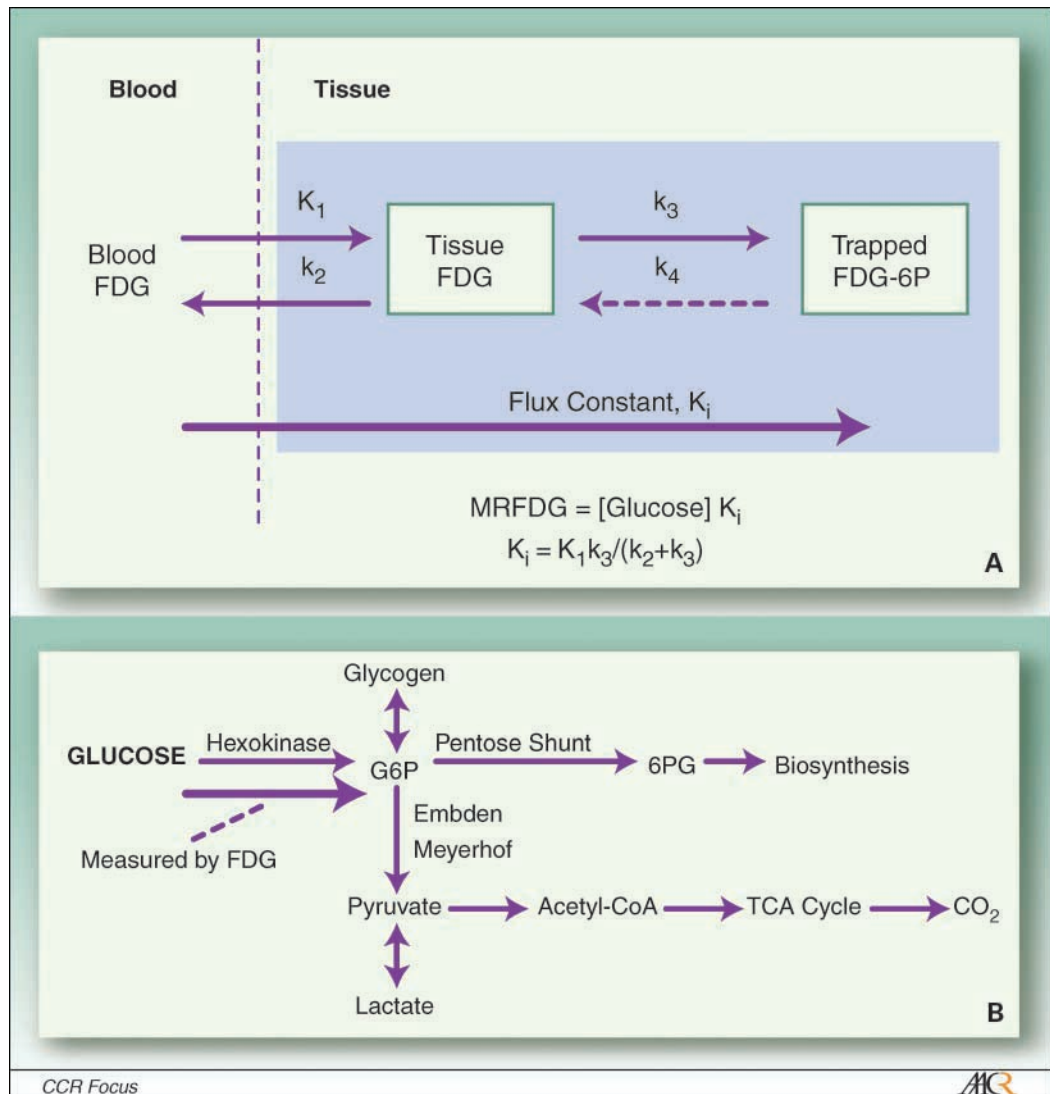
FDG PET for tumor detection. FDG PET is widely used for cancer detection, mostly for staging the extent of spread of newly diagnosed or recurrent cancers (3). The cancer types to which PET is most commonly applied include lung, breast, colorectal, lymphoma, melanoma, head and neck, sarcoma, cervical, thyroid, and esophageal cancers (3, 8, 24, 49). There is a wide range of FDG uptake in different tumors. Some tumors, such as lung, melanoma, and aggressive lymphoma, have reliably elevated FDG uptake compared with background in the untreated state (8, 24, 50). Others, such as early prostate cancer and well-differentiated hepatoma, have consistently low uptake; therefore, FDG PET has not proven useful for cancer detection and staging (51, 52). Yet others, such as breast, sarcoma, and thyroid, display a range of FDG uptake, which seems to depend on incompletely understood biological factors (53–56).

One emerging concept is that aberrant glycolysis, and therefore level of FDG uptake, is a marker of tumor dedifferentiation compared with the host tissue. For example, prostate and thyroid cancers that retain their endocrine function (androgen responsiveness and iodine avidity, respectively) have low FDG uptake; however, the dedifferentiated forms (androgen-refractory prostate cancer and iodine-negative thyroid cancer) are much more likely to be visualized by FDG PET (57, 58). Most studies suggest that FDG is not related in a simple way to tumor biological factors, suggesting that FDG PET provides an independent measure of *in vivo* tumor biology, distinct from *in vitro* assays (54).

Because accelerated energy metabolism is not specific to cancer, many noncancerous tissues will take up FDG, and false-positive findings are relatively common (59, 60). Causes of false-positive FDG uptake for tumor detection applications include inflammation, metabolism in musculoskeletal tissues and brown fat, and functional changes in response to stimulating agents, such as marrow-stimulating cytokines. Although the combination of PET and CT in PET/CT devices adds specificity to the scanning process, sites of uptake unrelated to cancer are common; therefore, considerable experience is necessary to properly interpret clinical FDG PET or PET/CT scans. Overall, low sensitivity for early-stage disease and modest specificity limit the utility of FDG PET for cancer screening and early diagnosis. However, FDG PET can be extraordinarily helpful in appropriately selected patients with an established cancer diagnosis, or strong suspicion of cancer, to characterize the disease and determine its extent.

FDG PET for monitoring tumor response. The application of FDG PET to clinical response monitoring has evolved somewhat more slowly than its use for staging and is currently approved for reimbursement for this purpose in the United States only for breast cancer (3). The earliest published studies using FDG PET to monitor therapeutic response by Minn and Wahl (17, 61) focused on advanced breast cancer treated with chemotherapy and compared imaging results with response by histopathology. These early studies showed that responders had a ~50% decline in FDG uptake 2 months into chemotherapy, whereas nonresponders had an insignificant decline (17). Subsequent studies done in a variety of cancers treated with a

Fig. 2. Model of FDG kinetics for estimating glycolytic flux in tissues. *A*, diagram of compartmental model of FDG kinetics. *B*, diagram of biochemical pathways in glucose metabolism. Bold arrow, portion measured by FDG PET.



variety of modalities support the utility of FDG PET for response monitoring and show that serial FDG PET predicts tumor response and in many cases patient outcome, such as disease-free survival (3, 12, 13, 21, 22, 24).

The timing and extent of the change in FDG uptake in response to treatment may vary with tumor type and importantly with the treatment. For cytotoxic chemotherapy, studies in breast cancer, lymphoma, gastrointestinal cancers, and others show the ability of FDG PET to discern response following a single cycle of chemotherapy (12–17). The precise biological factor associated with FDG decline after cytotoxic chemotherapy is unknown and is undoubtedly related to both a decline in the number of viable tumor cells and the rate of glucose consumption per cell. Early data in patients using FDG and thymidine PET suggested that declines in tumor proliferation precede changes in glycolysis (15). Recent data using drugs targeted to growth factor pathways up-regulated in some tumors, such as imatinib to inhibit the c-kit pathway in the treatment of gastrointestinal stromal tumor, suggest that

alterations in glycolysis, and therefore FDG uptake, occur within 1 to 2 days of starting treatment (Fig. 3; refs. 62–65). In this case, changes in FDG uptake may precede changes in tumor proliferation and cell death (66). The exact mechanism of this early change is unknown, but some recent studies implicate a rapid decline in glucose transporter expression (66); however, studies are needed to elucidate the precise mechanisms underlying changes in FDG PET as an indication of early response to this class of drugs (42). Glycolysis changes may also occur early in other forms of targeted therapy. For example, Mortimer et al. (29) found that an increase in FDG uptake 1 to 2 weeks after starting tamoxifen predicted subsequent breast cancer response. This FDG increase was interpreted as an indication of the early agonist or “flare” associated with tamoxifen therapy.

Measuring the response to radiotherapy remains more problematic in that FDG uptake may not decline after radiotherapy and may in fact increase early after treatment (67). The mechanism underlying these findings is speculated to be associated with a different and more prolonged period of

Downloaded from <http://aacrjournals.org/clinccancerres/article-pdf/13/12/3460/1969697/3460.pdf> by guest on 21 July 2024

cell viability and attempted repair before cell death for radiotherapy versus chemotherapy or possibly an inflammatory response to radiotherapy. In some studies, an increase in FDG uptake at the tumor site after radiotherapy predicted a better outcome. Spence et al. (23) found that an increase in FDG uptake after radiotherapy of high-grade gliomas portended better survival than an early decrease.

Some caution is needed in interpreting response data from FDG PET, as results may vary depending on the tumor, treatment, and time of assessment after therapy. Most data on response evaluation using FDG PET have come from small trials comparing PET results with standard size-based criteria or to pathology. A smaller number of studies have compared FDG PET results for therapy monitoring with more robust and more relevant end points, such as time-to-progression, disease-free survival, and overall survival. In those trials where this has been studied, serial FDG PET measures have been highly predictive of patient outcomes (13, 21, 55, 68–70). Currently, FDG PET is not as commonly used for response evaluation as it is for detection and staging. For response, FDG PET is most commonly used in lymphoma and breast cancer, where it has approval for Medicare payment for response evaluation. Emerging and increasingly used indications include response evaluation in head and neck cancer, sarcoma, lung cancer, and other tumors (67). Overall, FDG PET may be extremely helpful for evaluating response, and this indication should increase when prospective multicenter trials validate the predictive capability of serial FDG PET over the course of therapy. These studies need to consider carefully the timing of posttherapy imaging, and the imaging study needs to be quantified using measures such as SUV or metabolic rate of FDG. Such trials are under way for some tumor types (e.g., lymphoma; ref. 71).

Biological insights from FDG PET. In addition to its clinical role for cancer, FDG PET has provided some insights into *in vivo* tumor biology. The ability to characterize tumor glycolysis *in vivo* has shown that tumors are unusually glycolytic, out of proportion to metabolic needs for energy generation (41). Using combined imaging with [¹¹C]glucose and FDG, Spence et al. (46) showed that the relative utilization of glucose and FDG was different in brain tumors versus normal brain, which suggested different enzymology and/or pathway utilization. Whereas blood flow and glucose metabolism are typically quite tightly coupled in normal tissues, Tseng et al. (48) showed that they were uncoupled in untreated breast cancer and that effective treatment brought the pattern of tumor glucose metabolism closer to that of normal breast. These studies used FDG PET in conjunction with other PET radiopharmaceuticals and have suggested not only that the glycolytic rate elevated in tumors compared with normal tissue but also that the kinetics of glycolysis is aberrant in tumors compared with normal tissues, further refining the nature of the Warburg effect.

A striking feature of the FDG PET cancer literature is the prognostic capability of FDG. A high metabolic rate indicated by high FDG uptake seems to be an almost universal predictor of poor outcome for many tumor types, including lung cancer, breast cancer, sarcoma, lymphoma, glioma, and thyroid cancer (27, 55, 72–76). This remarkable predictive capability applies to a wide range of tumors treated in quite different ways, from primary surgery (lung) to primary chemotherapy and radiotherapy (lymphoma), to surgery plus chemotherapy (breast and high-grade sarcoma), to surgery plus external beam radiotherapy and chemotherapy (glioma), and to surgery plus radionuclide therapy (thyroid cancer). This predictive capability may stem from the fact that elevated glycolysis accompanies

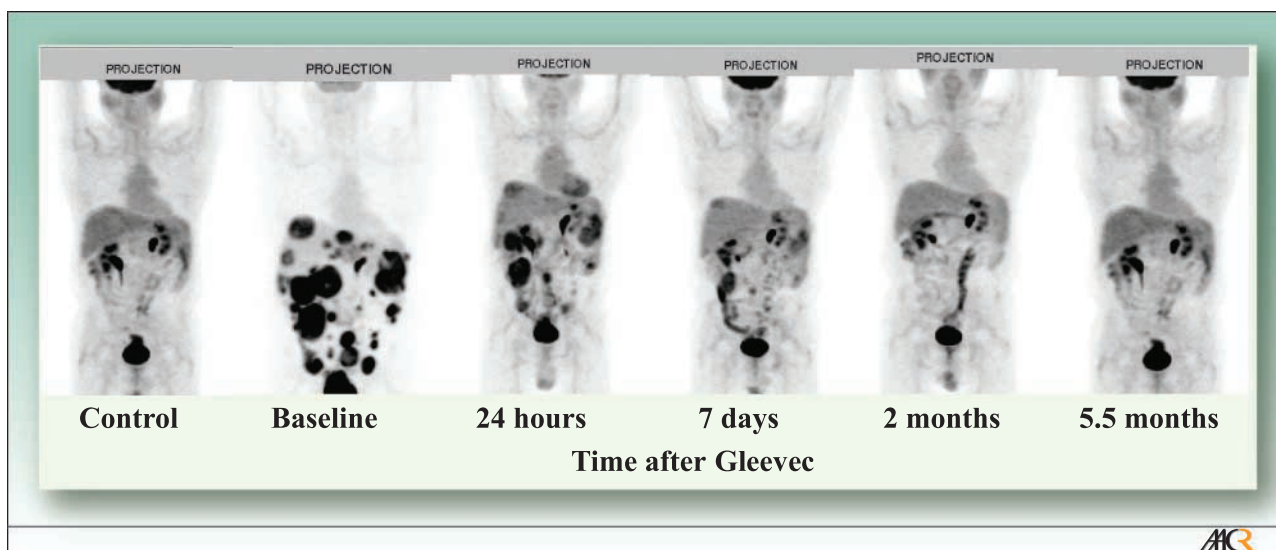


Fig. 3. FDG PET imaging of gastrointestinal stromal tumor before and after treatment. In patients with gastrointestinal stromal tumors, tumor glucose utilization is very high and these tumors can be readily visualized by [¹⁸F]FDG PET. A striking observation in patients with gastrointestinal stromal tumor who are treated with STI571 (Gleevec) was the rapid and sustained decrease in FDG uptake determined by PET scan that was seen as early as 24-h one dose of STI571, and this was sustained over many months. The high FDG levels seen in the kidney, ureter, and bladder are normal in both the pre-Gleevec and post-Gleevec images. Adapted with permission from Van den Abbeele et al., 2001.

several tumor and microenvironmental factors that have been associated with poor prognosis, including accelerated proliferation (77), tumor hypoxia (78–80), and diminished apoptosis (44, 45, 81). In some tumors (e.g., iodine-refractory thyroid cancer), FDG PET can be helpful in predicting tumor aggressiveness and identifying which patients need the most aggressive treatment (27, 58).

Beyond FDG

Although FDG continues to play an increasingly important role in the clinical management of cancer, it is likely that other PET radiopharmaceuticals will also contribute in the near future. FDG PET has important limitations, including the ability to detect small-volume disease, early tumors, and less aggressive and/or less glycolytic tumors. In some cases (e.g., in routine staging of early disease for many cancers), the use of FDG PET may not be helpful. Energy metabolism is associated with tumor growth, but also with a variety of other biological processes, including inflammation and tissue repair in response to damage (4, 82). As cancer treatment becomes more targeted and individualized to patient and tumor characteristics, more specific PET radiopharmaceuticals will help guide treatment selection by (a) quantifying the therapeutic target, (b) identifying resistance factors, and (c) measuring early response to therapy (6). These applications are highlighted below, with specific examples of the use of PET for each task. This is not intended as a comprehensive review of new cancer imaging approaches, for which the reader is referred to other recent reviews (1, 2, 4, 5). We have concentrated this review on ^{18}F -labeled PET agents and novel indications that are likely to have near-term clinical utility.

Quantifying the therapeutic target. The trend toward more specific therapy requires the ability to measure the level of target expression in the tumor. Current examples of specific targets (and examples of treatments directed at them) include the ER (tamoxifen and letrozole), HER2 (trastuzumab), epidermal growth factor receptor (gefitinib), and angiogenesis (bevacizumab; ref. 83). Measuring the target expression at each site of disease is a task for which PET is ideally suited. PET imaging can determine whether the target is expressed at all disease sites and can quantify the level of target expression at each site. Current examples of PET imaging to measure target expression include ER and androgen receptor imaging (84, 85); HER2 imaging (86); imaging angiogenesis nonspecifically by measuring blood flow (72, 87, 88) and by imaging specific components expressed in neovasculature (89–91); and measuring novel targets such as matrix metalloproteinases (92). In the future, it may also be possible to measure target expression in conjunction with gene therapy using a transgene imaging reporter (93).

PET imaging of ER expression in breast cancer provides a good example of how imaging to identify target expression can be helpful. ER expression in breast cancer is an indicator of prognosis and predicts the likelihood of responding to antiestrogen therapy. Assessment of ER expression in primary breast cancer by *in vitro* assay of biopsy material by immunohistochemistry is part of the standard care of breast

cancer patients and weighs heavily in the choice of therapy (94). A variety of agents has been tested for PET ER imaging (95). A close analogue of estradiol, the labeled estrogen, [^{18}F]16 α -17 β -fluoroestradiol, has shown the most promise in quantifying the functional ER status of breast cancer, either in the primary tumor or in the metastatic lesions (95). The quantitative level of FES uptake in primary tumors correlates with the level of ER expression measured by *in vitro* assay by radioligand binding (96) and, in preliminary data from our laboratory, by immunohistochemistry. FES PET provides sufficient image quality to image metastatic lesions with high sensitivity in patients with ER-positive tumors (84) at an acceptable radiation dose to the patient (97).

An important use of FES PET will be to image and characterize the entire volume of disease in an individual patient, especially in patients with recurrent or metastatic breast cancer, where tissue sampling at all sites is not feasible. Studies using FES PET have shown heterogeneous FES uptake within the same tumor and between different metastatic lesions (84). PET ER imaging can be used, in analogy to assay of ER in biopsy specimens, to predict the likelihood of response to hormonal therapy and thereby guide appropriate selection of patients for this type of treatment (Fig. 4). Studies by Mortimer et al. (29) have shown that a high level of FES uptake in advanced tumors predicts a greater likelihood of response to tamoxifen. Recent results from our center show similar results for patients with recurrent or metastatic breast cancer treated with a variety of hormonal agents (28). These preliminary results show the exciting potential of PET ER imaging to help guide appropriate, individualized breast cancer treatment and point the way for future clinical use.

Identifying resistance factors. Even when a tumor expresses appropriate levels of the target, targeted therapy may fail if the tumor also has characteristics that render it resistant to treatment. Preliminary tests of PET agents for specific resistance factors have been undertaken in animal models and are beginning in patients. The ability to measure both the therapeutic target and the specific resistance factors underlies the emerging role of PET in early drug testing (98).

Tumor hypoxia imaging with PET has received considerable attention and has been used in patients for several tumors (78). Tumor hypoxia has been well established as a resistance factor for radiotherapy, but evolving evidence indicates that it promotes tumor aggressiveness via genomic changes that lead to resistance to a variety of therapies (99). Although hypoxia likely contributes to increased rates of glycolysis and up-regulation of GLUT transporters, hypoxia cannot be inferred by FDG PET. Rajendran (100) showed, for patients with a variety of tumor types, that hypoxia could not be predicted by FDG uptake. Several PET agents specifically designed to image tumor hypoxia have been tested for hypoxia imaging (78). Of these, [^{18}F]fluoromisonidazole (FMISO) has the largest body of preclinical validation studies and clinical experience (78), although other PET hypoxia tracers have also been studied in patients (101). Recent studies have shown that tumor hypoxia measured by PET is highly predictive of patient outcome; patients with hypoxia by PET had considerably earlier relapse or progression (79, 101, 102). PET hypoxia imaging may provide a means for selecting alternative therapeutic strategies

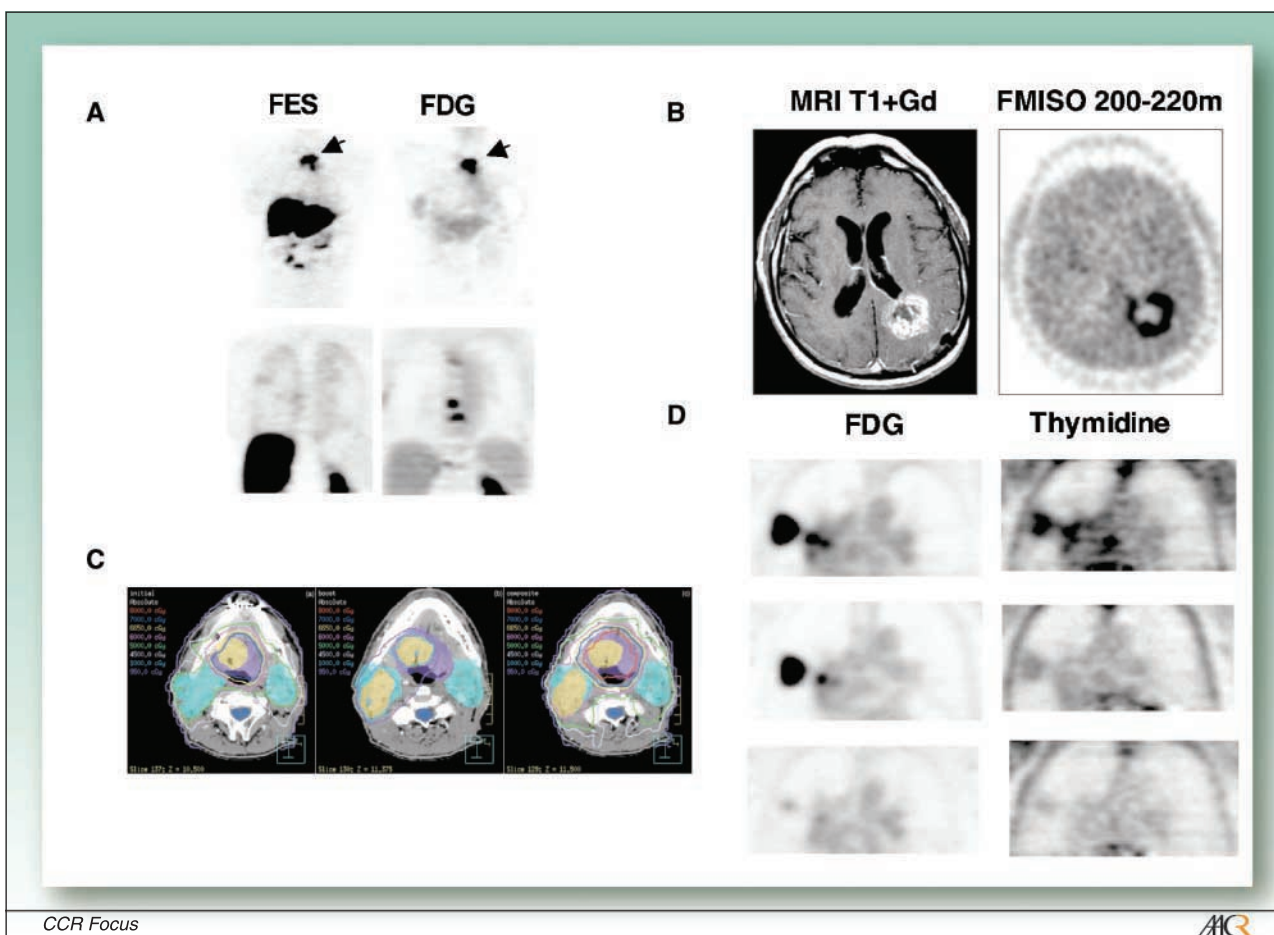


Fig. 4. Examples of applications of PET to direct cancer therapy. *A*, FDG and FES PET for two different patients (*top* and *bottom*) show the ability to image target expression, in this case the ER for breast cancer. Both patients had ER-expressing primary tumors; however, only the top patient had FES uptake in site of bone metastasis. The top patient had an excellent response to letrozole, whereas the bottom patient failed multiple endocrine therapies. *B*, FMISO PET of a recurrent glioblastoma after initial resection and treatment. FMISO uptake at sites of tumor recurrence seen on magnetic resonance imaging (*MRI*) portended a resistant and aggressive tumor, and the patients had limited subsequent survival. *C*, FMISO PET fused with CT images can be used to direct targeted radiotherapy by conformal treatments. Fused images show isodose lines for planned treatment and show how combined anatomic/metabolic imaging can direct target therapy. *D*, FDG and thymidine PET for a patient with a large lung cancer image pretherapy (*top*) and sequentially after chemoradiation (*middle* and *bottom*). The patient had a significant partial response to treatment, which was shown earlier by thymidine proliferation imaging than by FDG PET, and both preceded changes in size by CT.

in tumors resistant to standard treatments based on hypoxia and may direct patients to regional therapy and/or agents that are selective for hypoxic tissue (Fig. 4; refs. 79, 103).

Another area of active investigation in patients has been characterization of drug efflux proteins, in particular P-glycoprotein, which is a membrane transport protein for which several xenobiotics (104) are substrates. P-glycoprotein may mediate the enhanced efflux of several chemotherapeutic agents, including agents like doxorubicin and Taxol that are important in cancer treatment. Based on observations by Piwnica-Worms et al. (105), Ciarmiello et al. (106) observed that enhanced washout of the single-photon emission computed tomography agent, ^{99m}Tc-sestamibi (MIBI) predicted resistance to epirubicin-based therapy of locally advanced breast cancer. However, interpretation of MIBI images is confounded by blood flow, which is another important factor in the uptake and washout of MIBI (107). Alternative PET radiotracers, such as [¹¹C]verapamil have been developed as

agents for imaging P-glycoprotein transport (108). We have shown recently that verapamil PET can be used to measure the effect of P-glycoprotein inhibition on drug transport into the brain (109). Measurements of P-glycoprotein transport have also been done using ¹⁸F-labeled agents, such as [¹⁸F]fluoropaclitaxel (110).

Measuring early response. As the choice of cancer treatments expands, there will be an increasing need to measure the efficacy of treatments as early as possible after initiation. With many potentially effective treatments to choose from, it will be important to identify ineffective treatments early for the individual patient. Some new therapies, such as antiangiogenesis agents, may be cytostatic instead of cytoreductive, in which case successful treatment may not lead to a decrease in tumor size. Studies of FDG PET after a single dose of chemotherapy have supported the ability of *in vivo* biochemical imaging to measure early response (14, 16), although as described earlier, changes in FDG uptake with early response

may differ for different tumors and treatments. It is likely that other imaging agents that more directly measure cell growth and death will be even more effective at measuring early response.

Decreased tumor proliferation is an early event in response to successful treatment (111). This idea underlies the use of labeled thymidine and analogues to image cellular proliferation and early response to treatment (112). Thymidine is incorporated into DNA but not RNA; therefore, thymidine uptake and retention in the tumor serves as a specific marker of cell growth (111). Recent studies using [^{11}C]thymidine and PET show promise in assessing response, especially early response as reviewed by Mankoff et al. (112). Because of the short half-life of ^{11}C (~20 min) and its rapid metabolism to thymine and other metabolites, [^{11}C]thymidine is not practical for routine clinical use outside of academic centers. This problem spurred the development of ^{18}F -labeled, nonmetabolized thymidine analogues to image tumor proliferation. The most promising thus far is [^{18}F]fluorothymidine (FLT; ref. 113). Studies in several tumor types have shown that FLT uptake correlates with *in vitro* measures of proliferation done on biopsy specimens (reviewed in ref. 112). Several laboratories have ongoing studies using FLT PET to measure response in several different tumor types (114). However, as with FDG, the image of FLT is confounded by transport limitations, unphosphorylated FLT in tissue, and release of phosphorylated FLT from tissue (115, 116). It is important to analyze FLT images quantitatively to measure these kinetic effects before drawing conclusions about the meaning of FLT uptake in tumors, and there may be important differences between FLT and thymidine as markers of proliferation (33, 116, 117).

Besides an early decline in cell growth, effective treatments often lead to an early increase in cell death, often by apoptosis (81). Radiopharmaceuticals directed at phosphatidylserine residues that normally reside on the intracellular membrane surface but that are translocated to the extracellular surface during apoptosis have been developed for apoptosis imaging.

The single-photon emission computed tomography agent $^{99\text{m}}\text{Tc}$ -Annexin V has shown the ability to image apoptosis *in vivo*, but use of this metal-labeled agent was confounded by high background, including liver uptake (118). In early studies using this agent in patients undergoing cancer treatments, the level of uptake in $^{99\text{m}}\text{Tc}$ -Annexin V correlated with *in vitro* assay of apoptosis on biopsy material, but the level of uptake and target-to-background ratio were only modest (119). Concern has been expressed that the relatively small number of cells undergoing apoptosis at any one time and the small time window to have access to phosphatidylserine moieties during the apoptotic process (120) may limit the widespread use of Annexin V-based imaging. However, these same considerations may provide an advantage for mechanistic studies of early response that are important in determining optimal timing in multiagent therapy. Annexin tracers labeled for use in PET will offer better image quality, better quantification, and the ability to measure smaller quantities of radiopharmaceutical and have undergone preliminary validation in animals (121, 122). Alternate approaches to imaging apoptosis are also being explored (123). The ability to image both changes in cell proliferation and cell death in response to treatment will be an effective means of characterizing how tumors respond to targeted therapy.

Summary

Molecular and biochemical imaging by PET offers several significant advantages for cancer imaging. Almost all of the current clinical application of PET in cancer thus far uses FDG and focuses on cancer staging. Future applications of PET to cancer care will require further studies of FDG PET and radiopharmaceuticals beyond FDG, rigorous quantification, especially for response evaluation, and careful study design to validate the information provided by PET imaging compared with both *in vitro* assay and with well-defined patient outcomes.

References

- Blasburg R. Imaging update: new windows, new views. *Clin Cancer Res* 2007;13:3444–8.
- Jackson A, O'Connor J, Parker G, Jayson G. Imaging tumor vascular heterogeneity and angiogenesis using DCE-MRI. *Clin Cancer Res* 2007;13:3449–59.
- Kelloff GJ, Hoffman JM, Johnson B, et al. Progress and promise of FDG-PET imaging for cancer patient management and oncologic drug development. *Clin Cancer Res* 2005;11:2785–808.
- Kelloff GJ, Krohn KA, Larson SM, et al. The progress and promise of molecular imaging probes in oncologic drug development. *Clin Cancer Res* 2005;11:7967–85.
- Wester HJ. Nuclear imaging probes: from bench to bedside. *Clin Cancer Res* 2007;13:3476–81.
- Mankoff DA, Krohn KA. PET imaging of response and resistance to cancer therapy. In: Teicher B, editor. *Drug resistance in cancer*. Totowa (NJ): Humana Press; 2006. p. 105–22.
- Eubank WB, Mankoff DA, Schmiedl UP, et al. Imaging of oncologic patients: benefit of combined CT and FDG PET in the diagnosis of malignancy. *AJR Am J Roentgenol* 1998;171:1103–10.
- Vansteenkiste JF. PET scan in the staging of non-small cell lung cancer. *Lung Cancer* 2003;42 Suppl 1: S27–37.
- Alessio AM, Kinahan PE, Cheng PM, Vesselle H, Karp JS. PET/CT scanner instrumentation, challenges, and solutions. *Radiol Clin North Am* 2004; 42:1017–32, vii.
- Husband JE. Monitoring tumor response. *Eur Radiol* 1996;6:775–85.
- Therasse P, Arbuick SG, Eisenhauer EA, et al.; European Organization for Research and Treatment of Cancer, National Cancer Institute of the United States, National Cancer Institute of Canada. New guidelines to evaluate the response to treatment in solid tumors. *J Natl Cancer Inst* 2000;92:205–16.
- Ott K, Weber WA, Lordick F, et al. Metabolic imaging predicts response, survival, and recurrence in adenocarcinomas of the esophagogastric junction. *J Clin Oncol* 2006;24:4692–8.
- Romer W, Hanauske AR, Ziegler S, et al. Positron emission tomography in non-Hodgkin's lymphoma: assessment of chemotherapy with fluorodeoxyglucose. *Blood* 1998;91:4464–71.
- Schelling M, Avril N, Nahrig J, et al. Positron emission tomography using [^{18}F] fluorodeoxyglucose for monitoring primary chemotherapy in breast cancer. *J Clin Oncol* 2000;18:1689–95.
- Shields AF, Mankoff DA, Link JM, et al. Carbon-11-thymidine and FDG to measure therapy response. *J Nucl Med* 1998;39:1757–62.
- Smith I, Welch A, Hutcheon A, et al. Positron emission tomography using [^{18}F] fluorodeoxy-D-glucose to predict the pathologic response of breast cancer to primary chemotherapy. *J Clin Oncol* 2000;18: 1676–88.
- Wahl RL, Zasadny K, Helvie M, et al. Metabolic monitoring of breast cancer chemohormonotherapy using positron emission tomography: initial evaluation. *J Clin Oncol* 1993;11:2101–11.
- Nasr A, Stulberg J, Weitzman S, Gerstle JT. Assessment of residual posttreatment masses in Hodgkin's disease and the need for biopsy in children. *J Pediatr Surg* 2006;41:972–4.
- Hoekstra CJ, Pagliani I, Hoekstra OS, et al. Monitoring response to therapy in cancer using [^{18}F]-2-fluoro-2-deoxy-D-glucose and positron emission to-

- mography: an overview of different analytical methods. *Eur J Nucl Med* 2000;27:731–43.
20. Lammertsma AA. Measurement of tumor response using [¹⁸F]-2-fluoro-2-deoxy-D-glucose and positron-emission tomography. *J Clin Pharmacol* 2001;41: Suppl:104–6S.
 21. Mac Manus MP, Hicks RJ, Matthews JP, et al. Positron emission tomography is superior to computed tomography scanning for response-assessment after radical radiotherapy or chemoradiotherapy in patients with non-small-cell lung cancer. *J Clin Oncol* 2003;21: 1285–92.
 22. Mankoff DA, Dunnwald LK, Gralow JR, et al. Changes in blood flow and metabolism in locally advanced breast cancer treated with neoadjuvant chemotherapy. *J Nucl Med* 2003;44:1806–14.
 23. Spence AM, Muzi M, Graham MM, et al. 2-[(18)F]Fluoro-2-deoxyglucose and glucose uptake in malignant gliomas before and after radiotherapy: correlation with outcome. *Clin Cancer Res* 2002;8: 971–9.
 24. Weber WA, Petersen V, Schmidt B, et al. Positron emission tomography in non-small-cell lung cancer: prediction of response to chemotherapy by quantitative assessment of glucose use. *J Clin Oncol* 2003; 21:2651–7.
 25. Weber WA. Positron emission tomography as an imaging biomarker. *J Clin Oncol* 2006;24:3282–92.
 26. Hartwell L, Mankoff D, Paulovich A, Ramsey S, Swisher E. Cancer biomarkers: a systems approach. *Nat Biotechnol* 2006;24:905–8.
 27. Robbins RJ, Wan Q, Grewal RK, et al. Real-time prognosis for metastatic thyroid carcinoma based on 2-[(18)F]fluoro-2-deoxy-D-glucose-positron emission tomography scanning. *J Clin Endocrinol Metab* 2006;91:498–505.
 28. Linden HM, Stehova SA, Link JM, et al. Quantitative fluorodeoxyglucose positron emission tomography imaging predicts response to endocrine treatment in breast cancer. *J Clin Oncol* 2006;24: 2793–9.
 29. Mortimer JE, Dehdashti F, Siegel BA, Trinkaus K, Katzenellenbogen JA, Welch MJ. Metabolic flare: indicator of hormone responsiveness in advanced breast cancer. *J Clin Oncol* 2001;19:2797–803.
 30. Sokoloff L, Reivich M, Kennedy C, et al. The [¹⁴C]deoxyglucose method for the measurement of local cerebral glucose utilization: theory, procedure, and normal values in the conscious and anesthetized albino rat. *J Neurochem* 1977;28:897–916.
 31. Phelps M, Huang S, Hoffman E. Tomographic measurement of local cerebral glucose metabolic rate in humans with (18F)2-fluoro-2-deoxy-D-glucose: validation of method. *Ann Neurol* 1979;6:371.
 32. Reivich M, Kuhl D, Wolf A, et al. The [¹⁸F]fluoro-deoxyglucose method for the measurement of local cerebral glucose utilization in man. *Circ Res* 1979;44: 127–37.
 33. Krohn KA, Mankoff DA, Muzi M, Link JM, Spence AM. True tracers: comparing FDG with glucose and FLT with thymidine. *Nucl Med Biol* 2005;32: 663–71.
 34. Huang S-C. Anatomy of SUV. *Nucl Med Biol* 2000; 27:643–6.
 35. Shankar LK, Hoffman JM, Bacharach S, et al. Consensus recommendations for the use of ¹⁸F-FDG PET as an indicator of therapeutic response in patients in National Cancer Institute Trials. *J Nucl Med* 2006;47: 1059–66.
 36. Zasadny KR, Wahl RL. Standardized uptake values of normal tissues at PET with 2-[fluorine-18]-fluoro-2-deoxy-D-glucose: variations with body weight and a method for correction. *Radiology* 1993;189: 847–50.
 37. Warburg O. The metabolism of tumors. New York: Richard R. Smith; 1931.
 38. Spence AM, Graham MM, Muzi M, et al. Feasibility of imaging pentose cycle glucose metabolism in gliomas with PET: studies in rat brain tumor models. *J Nucl Med* 1997;38:617–24.
 39. Clavo AC, Brown RS, Wahl RL. Fluorodeoxyglucose uptake in human cancer cell lines is increased by hypoxia. *J Nucl Med* 1995;36:1625–32.
 40. Mathapala S, Rempel A, Pederson P. Aberrant glycolytic metabolism of cancer cells: a remarkable coordination of genetic, transcriptional, post-translational, and mutational events that lead to a critical role for type II hexokinase. *J Bioenerg Biomembr* 1997;29: 339–43.
 41. Gatenby RA, Gillies RJ. Why do cancers have high aerobic glycolysis? *Nat Rev Cancer* 2004;4:891–9.
 42. Linden HM, Krohn KA, Livingston RB, Mankoff DA. Monitoring targeted therapy: is fluorodeoxyglucose uptake a marker of early response? *Clin Cancer Res* 2006;12:5608–10.
 43. Sebolt-Leopold JS, Herrera R. Targeting the mitogen-activated protein kinase cascade to treat cancer. *Nat Rev Cancer* 2004;4:937–47.
 44. Thompson JE, Thompson CB. Putting the rap on Akt. *J Clin Oncol* 2004;22:4217–26.
 45. Brand K. Aerobic glycolysis by proliferating cells: protection against oxidative stress at the expense of energy yield. *J Bioenerg Biomembr* 1997;29: 335–64.
 46. Spence AM, Muzi M, Graham MM, et al. Glucose metabolism in human malignant gliomas measured quantitatively with PET, 1-[C-11]glucose, and FDG: analysis of the FDG lumped constant. *J Nucl Med* 1998;39:440–8.
 47. Aloj L, Caraco C, Jagoda E, Eckelman WC, Neumann RD. Glut-1 and hexokinase expression: relationship with 2-fluoro-2-deoxy-D-glucose uptake in A31 and T47D cells in culture. *Cancer Res* 1999;59: 4709–17.
 48. Tseng J, Dunnwald LK, Schubert EK, et al. ¹⁸F-FDG kinetics in locally advanced breast cancer: correlation with tumor blood flow and changes in response to neoadjuvant chemotherapy. *J Nucl Med* 2004;45: 1829–37.
 49. Eubank W, Mankoff D. Current and future uses of PET in breast cancer imaging. *Semin Nucl Med* 2004;34:224–40.
 50. Macapinlac HA. FDG PET and PET/CT imaging in lymphoma and melanoma. *Cancer J* 2004;10: 262–70.
 51. Hoh CK, Seltzer MA, Franklin J, deKernion JB, Phelps ME, Belldgrun A. Positron emission tomography in urological oncology. *J Urol* 1998;159: 347–56.
 52. Khan MA, Combs CS, Brunt EM, et al. Positron emission tomography scanning in the evaluation of hepatocellular carcinoma. *J Hepatol* 2000;32:792–7.
 53. Avril N, Menzel M, Dose J, et al. Glucose metabolism of breast cancer assessed by ¹⁸F-FDG PET: histologic and immunohistochemical tissue analysis. *J Nucl Med* 2001;42:9–16.
 54. Bos R, van Der Hoeven JJ, van Der Wall E, et al. Biologic correlates of (18)fluorodeoxyglucose uptake in human breast cancer measured by positron emission tomography. *J Clin Oncol* 2002;20:379–87.
 55. Eary JF, O'Sullivan F, Powitan Y, et al. Sarcoma tumor FDG uptake measured by PET and patient outcome: a retrospective analysis. *Eur J Nucl Med Mol Imaging* 2002;29:1149–54.
 56. Wang W, Larson SM, Fazzari M, et al. Prognostic value of [¹⁸F]fluorodeoxyglucose positron emission tomographic scanning in patients with thyroid cancer. *J Clin Endocrinol Metab* 2000;85:1107–13.
 57. Morris MJ, Akhurst T, Osman I, et al. Fluorinated deoxyglucose positron emission tomography imaging in progressive metastatic prostate cancer. *Urology* 2002;59:913–8.
 58. Wang W, Larson SM, Tuttle RM, et al. Resistance of [¹⁸F]-fluorodeoxyglucose-avid metastatic thyroid cancer lesions to treatment with high-dose radioactive iodine. *Thyroid* 2001;11:1169–75.
 59. Mankoff D, Bellon J. PET imaging of cancer: FDG and beyond. *Semin Radiat Oncol* 2001;11:16–27.
 60. Rohren EM, Turkington TG, Coleman RE. Clinical applications of PET in oncology. *Radiology* 2004; 231:305–32.
 61. Minn H, Soini I. [¹⁸F]fluorodeoxyglucose scintigraphy in diagnosis and follow up of treatment in advanced breast cancer. *Eur J Nucl Med* 1989;15:61–6.
 62. Demetri GD, von Mehren M, Blanke CD, et al. Efficacy and safety of imatinib mesylate in advanced gastrointestinal stromal tumors. *N Engl J Med* 2002; 347:472–80.
 63. Gayed I, Vu T, Iyer R, et al. The role of [¹⁸F]-FDG PET in staging and early prediction of response to therapy of recurrent gastrointestinal stromal tumors. *J Nucl Med* 2004;45:17–21.
 64. Stroobants S, Goeminne J, Seegers M, et al. ¹⁸FDG-positron emission tomography for the early prediction of response in advanced soft tissue sarcoma treated with imatinib mesylate (Glivec). *Eur J Cancer* 2003; 39:2012–20.
 65. Van den Abbeele AD, Group ftGCPS. [F-18]-FDG in PET provides early evidence of biological response to ST1571 in patients with malignant gastrointestinal stromal tumors (GIST). *Proc Am Soc Clin Oncol* 2001;20:362a.
 66. Su H, Bodenstein C, Dumont RA, et al. Monitoring tumor glucose utilization by positron emission tomography for the prediction of treatment response to epidermal growth factor receptor kinase inhibitors. *Clin Cancer Res* 2006;12:5659–67.
 67. Hicks RJ. The role of PET in monitoring therapy. *Cancer Imaging* 2005;5:51–7.
 68. Cachin F, Prince HM, Hogg A, Ware RE, Hicks RJ. Powerful prognostic stratification by [¹⁸F]fluorodeoxyglucose positron emission tomography in patients with metastatic breast cancer treated with high-dose chemotherapy. *J Clin Oncol* 2006;24:3026–31.
 69. Hawkins DS, Schuetze SM, Butrynski JE, et al. [¹⁸F]Fluorodeoxyglucose positron emission tomography predicts outcome for Ewing sarcoma family of tumors. *J Clin Oncol* 2005;23:8828–34.
 70. Specht JM, Tam SL, Kurland BF, et al. Serial 2-[(18)F] fluoro-2-deoxy-D- -glucose positron emission tomography (FDG-PET) to monitor treatment of bone-dominant metastatic breast cancer predicts time to progression (TTP). *Breast Cancer Res Treat*. Epub 2007 Feb 10.
 71. Juweid ME, Stroobants S, Hoekstra OS, et al. Use of positron emission tomography for response assessment of lymphoma: consensus of the Imaging Subcommittee of International Harmonization Project in Lymphoma. *J Clin Oncol* 2007;25:571–8.
 72. Mankoff DA, Dunnwald LK, Gralow JR, et al. Blood flow and metabolism in locally advanced breast cancer: relationship to response to therapy. *J Nucl Med* 2002;43:500–9.
 73. Oshida M, Uno K, Suzuki M, et al. Predicting the prognoses of breast carcinoma patients with positron emission tomography using 2-deoxy-2-fluoro [¹⁸F]-D-glucose. *Cancer* 1998;82:2227–34.
 74. Patronas NJ, Di Chiro G, Kufta C, et al. Prediction of survival in glioma patients by means of positron emission tomography. *J Neurosurg* 1985;62:816–22.
 75. Tralins KS, Douglas JG, Stelzer KJ, et al. Volumetric analysis of ¹⁸F-FDG PET in glioblastoma multiforme: prognostic information and possible role in definition of target volumes in radiation dose escalation. *J Nucl Med* 2002;43:1667–73.
 76. Vansteenkiste J, Fischer BM, Doms C, Mortensen J. Positron-emission tomography in prognostic and therapeutic assessment of lung cancer: systematic review. *Lancet Oncol* 2004;5:531–40.
 77. Pinder SE, Wencyk P, Sibbering DM, et al. Assessment of the new proliferation marker MIB1 in breast carcinoma using image analysis: associations with other prognostic factors and survival. *Br J Cancer* 1995;71:146–9.

78. Rajendran JG, Krohn KA. Imaging hypoxia and angiogenesis in tumors. *Radiol Clin North Am* 2005;43:169–87.
79. Rischin D, Hicks RJ, Fisher R, et al. Prognostic significance of [¹⁸F]-misonidazole positron emission tomography-detected tumor hypoxia in patients with advanced head and neck cancer randomly assigned to chemoradiation with or without tirapazamine: a substudy of Trans-Tasman Radiation Oncology Group Study 98.02. *J Clin Oncol* 2006;24:2098–104.
80. Vaupel P. Tumor microenvironmental physiology and its implications for radiation oncology. *Semin Radiat Oncol* 2004;14:198–206.
81. Hockenbery D. Defining apoptosis. *Am J Pathol* 1995;146:16–9.
82. Krohn KA, Mankoff DA, Eary JF. Imaging cellular proliferation as a measure of response to therapy. *J Clin Pharmacol* 2001;41:96–103S.
83. Kaklamani V, O'Regan RM. New targeted therapies in breast cancer. *Semin Oncol* 2004;31:20–5.
84. Dehdashti F, Mortimer JE, Siegel BA, et al. Positron tomographic assessment of estrogen receptors in breast cancer: a comparison with FDG-PET and *in vitro* receptor assays. *J Nucl Med* 1995;36:1766–74.
85. Larson SM, Morris M, Gunther I, et al. Tumor localization of 16-¹⁸F-fluoro-5 α -dihydrotestosterone versus ¹⁸F-FDG in patients with progressive, metastatic prostate cancer. *J Nucl Med* 2004;45:366–73.
86. Gonzalez-Trotter DE, Manjeshwar RM, Doss M, et al. Quantitation of small-animal (124I) activity distributions using a clinical PET/CT scanner. *J Nucl Med* 2004;45:1237–44.
87. Wilson CB, Lammertsma AA, McKenzie CG, Sikora K, Jones T. Measurements of blood flow and exchanging water space in breast tumors using positron emission tomography: a rapid and non-invasive dynamic method. *Cancer Res* 1992;52:1592–7.
88. Zasadny KR, Tatsumi M, Wahl RL. FDG metabolism and uptake versus blood flow in women with untreated primary breast cancers. *Eur J Nucl Med Mol Imaging* 2003;30:274–80.
89. Beer AJ, Haubner R, Sarbia M, et al. Positron emission tomography using [¹⁸F]galacto-RGD identifies the level of integrin $\alpha(v)\beta_3$ expression in man. *Clin Cancer Res* 2006;12:3942–9.
90. Chen X, Sievers E, Hou Y, et al. Integrin $\alpha_v\beta_3$ -targeted imaging of lung cancer. *Neoplasia* 2005;7:271–9.
91. Haubner R, Wester HJ, Burkhart F, et al. Glycosylated RGD-containing peptides: tracer for tumor targeting and angiogenesis imaging with improved biokinetics. *J Nucl Med* 2001;42:326–36.
92. Zheng QH, Fei X, Liu X, et al. Synthesis and preliminary biological evaluation of MMP inhibitor radiotracers [¹¹C]methyl-halo-CGS 27023A analogs, new potential PET breast cancer imaging agents. *Nucl Med Biol* 2002;29:761–70.
93. Berger F, Gambhir SS. Recent advances in imaging endogenous or transferred gene expression utilizing radionuclide technologies in living subjects: applications to breast cancer. *Breast Cancer Res* 2001;3:28–35.
94. Sledge GJ, McGuire W. Steroid hormone receptors in human breast cancer. *Adv Cancer Res* 1983;38:61–75.
95. Katzenellenbogen JA, Welch MJ, Dehdashti F. The development of estrogen and progestin radiopharmaceuticals for imaging breast cancer. *Anticancer Res* 1997;17:1573–6.
96. Mintun MA, Welch MJ, Siegel BA, et al. Breast cancer: PET imaging of estrogen receptors. *Radiology* 1988;169:45–8.
97. Mankoff DA, Peterson LM, Tewson TJ, et al. [¹⁸F]fluoroestradiol radiation dosimetry in human PET studies. *J Nucl Med* 2001;42:679–84.
98. Aboagye EO, Price PM. Use of positron emission tomography in anticancer drug development. *Invest New Drugs* 2003;21:169–81.
99. Sutherland R. Tumor hypoxia and gene expression. *Acta Oncol* 1998;37:567–74.
100. Rajendran JG, Mankoff DA, O'Sullivan F, et al. Hypoxia and glucose metabolism in malignant tumors: evaluation by [¹⁸F]fluoromisonidazole and [¹⁸F]fluorodeoxyglucose positron emission tomography imaging. *Clin Cancer Res* 2004;10:2245–52.
101. Dehdashti F, Grigsby PW, Mintun MA, Lewis JS, Siegel BA, Welch MJ. Assessing tumor hypoxia in cervical cancer by positron emission tomography with 60Cu-ATSM: relationship to therapeutic response—a preliminary report. *Int J Radiat Oncol Biol Phys* 2003;55:1233–8.
102. Rajendran JG, Schwartz DL, O'Sullivan J, et al. Tumor hypoxia imaging with [F-18] fluoromisonidazole positron emission tomography in head and neck cancer. *Clin Cancer Res* 2006;12:5435–41.
103. Rajendran JG, Hendrickson KR, Spence AM, Muzi M, Krohn KA, Mankoff DA. Hypoxia imaging-directed radiation treatment planning. *Eur J Nucl Med Mol Imaging* 2006;33 Suppl 13:44–53.
104. Kaye SB. Multidrug resistance: clinical relevance in solid tumours and strategies for circumvention. *Curr Opin Oncol* 1998;10 Suppl 1:S15–9.
105. Piwnicka-Worms D, Chiu ML, Budding M, Kronauge JF, Kramer RA, Croop JM. Functional imaging of multidrug-resistant P-glycoprotein with an organotechnetium complex. *Cancer Res* 1993;53:977–84.
106. Ciarmiello A, Vecchio SD, Silvestro P, et al. Tumor clearance of technetium 99m-sestamibi as a predictor of response to neoadjuvant chemotherapy for locally advanced breast cancer. *J Clin Oncol* 1998;16:1677–83.
107. Mankoff DA, Dunnwald LK, Gralow JR, et al. [Tc-99m]-sestamibi uptake and washout in locally advanced breast cancer are correlated with tumor blood flow. *Nucl Med Biol* 2002;29:719–27.
108. Hendrikse NH, de Vries EG, Eriks-Fluks L, et al. A new *in vivo* method to study P-glycoprotein transport in tumors and the blood-brain barrier. *Cancer Res* 1999;59:2411–6.
109. Sasongko L, Link JM, Muzi M, et al. Imaging P-glycoprotein transport activity at the human blood-brain barrier with positron emission tomography. *Clin Pharmacol Ther* 2005;77:503–14.
110. Kurziel KA, Kieswetter do, Carson RE, Eckelman WC, Herscovitch P. Biodistribution, radiation dose estimates, and *in vivo* P-gp modulation studies of ¹⁸F-paclitaxel in nonhuman primates. *J Nucl Med* 2003;44:1330–9.
111. Cleaver JE. Thymidine metabolism and cell kinetics. *Frontiers Biol* 1967;6:43–100.
112. Mankoff DA, Shields AF, Krohn KA. PET imaging of cellular proliferation. *Radiol Clin North Am* 2005;43:153–67.
113. Grierson JR, Shileds AF. Radiosynthesis of 3'-deoxy-3'-[F-18]-fluorothymidine: [F-18]-FLT for imaging of cellular proliferation *in vivo*. *Nucl Med Biol* 2000;27:143–56.
114. Pio BS, Park CK, Satyamurthy N, Czernin J, Phelps ME, Silverman DH. PET with fluoro-L-thymidine allows early prediction of breast cancer response to chemotherapy. *J Nucl Med* 2003;44:76P.
115. Muzi M, Mankoff DA, Grierson JR, Wells JM, Vesselle H, Krohn KA. Kinetic modeling of 3'-deoxy-3'-fluorothymidine in somatic tumors: mathematical studies. *J Nucl Med* 2005;46:371–80.
116. Muzi M, Spence AM, O'Sullivan F, et al. Kinetic analysis of 3'-deoxy-3'-¹⁸F-fluorothymidine in patients with gliomas. *J Nucl Med* 2006;47:1612–21.
117. Wells JM, Mankoff DA, Eary JF, et al. Kinetic analysis of 2-[¹¹C]thymidine PET imaging studies of malignant brain tumors: preliminary patient results. *Mol Imaging* 2002;1:145–50.
118. Blankenberg F, Katsikis P, Tait J, et al. Imaging of apoptosis (programmed cell death) with 99mTc Annexin V. *J Nucl Med* 1999;40:184–91.
119. van de Wiele C, Lahorte C, Vermeersch H, et al. Quantitative tumor apoptosis imaging using technetium-99m-HYNIC Annexin V single photon emission computed tomography. *J Clin Oncol* 2003;21:3483–7.
120. Mandl SJ, Mari C, Edinger M, et al. Multi-modality imaging identifies key times for Annexin V imaging as an early predictor of therapeutic outcome. *Mol Imaging* 2004;3:1–8.
121. Collingridge DR, Glaser M, Osman S, et al. *In vitro* selectivity, *in vivo* biodistribution, and tumour uptake of Annexin V radiolabelled with a positron emitting radioisotope. *Br J Cancer* 2003;89:1327–33.
122. Yagle KJ, Eary JF, Tait JF, et al. Evaluation of ¹⁸F-Annexin V as a PET imaging agent in an animal model of apoptosis. *J Nucl Med* 2005;46:658–66.
123. Lahorte CM, Vanderheyden JL, Steinmetz N, Van de Wiele C, Dierckx RA, Slegers G. Apoptosis-detecting radioligands: current state of the art and future perspectives. *Eur J Nucl Med Mol Imaging* 2004;31:887–919.